arXiv:2410.14846v3 [astro-ph.GA] 2 Dec 2024

EARLY BRIGHT GALAXIES FROM HELIUM ENHANCEMENTS IN HIGH-REDSHIFT STAR CLUSTERS

Harley Katz[1,2], Alexander P. Ji[1,2], O. Grace Telford[3,4], & Peter Senchyna[4]

[1]Department of Astronomy & Astrophysics, University of Chicago, 5640 S Ellis Avenue, Chicago, IL 60637, USA
[2]Kavli Institute for Cosmological Physics, University of Chicago, Chicago, IL 60637, USA
[3]Department of Astrophysical Sciences, Princeton University, 4 Ivy Lane, Princeton, NJ 08544, USA and
[4]The Observatories of the Carnegie Institution for Science, 813 Santa Barbara Street, Pasadena, CA 91101, USA
Version December 3, 2024

ABSTRACT

The first few cycles of JWST have identified an overabundance of UV-bright galaxies and a general excess of UV luminosity density at $z \gtrsim 10$ compared to expectations from most (pre-JWST) theoretical models. Moreover, some of the brightest high-redshift spectroscopically confirmed galaxies exhibit peculiar chemical abundance patterns, most notably extremely high N/O ratios. Since N/O has been empirically shown to scale strongly with He/H, as expected for hot hydrogen burning, these same bright high-redshift galaxies are likely also helium-enhanced. Under simplistic assumptions for stellar evolution, the bolometric luminosity of a star scales as $L \propto (2 - \frac{5}{4}Y)^{-4}(2 - Y)^{-1}$ — hence a higher He/H leads to brighter stars. In this Letter, we evolve a series of MESA models to the zero-age main-sequence and highlight that the helium enhancements at the levels measured and inferred for high-redshift galaxies can boost the 1500 Å UV luminosity by up to $\sim 50\%$, while simultaneously increasing the stellar effective temperature. The combination of helium enhancements with nebular continuum emission expected for intense bursts of star formation have the potential to help reduce the tension between JWST observations and certain galaxy formation models.

1. INTRODUCTION

Photometric and spectroscopic measurements from JWST (Gardner et al. 2006) have demonstrated that there are both more UV-bright galaxies at high redshift and more generally an excess UV luminosity density compared to expectations from most pre-JWST theoretical models of high-redshift galaxy formation (e.g., Finkelstein et al. 2023; Harikane et al. 2024; Leung et al. 2023; Chemerynska et al. 2023, although cf. Willott et al. 2023). Numerous astrophysical solutions have been proposed to explain these observations that can be categorized as either (1) modifications to the observed mass-to-light ratio or (2) appealing to a higher star formation efficiency.

Within the first category, possible physical mechanisms that can impact the mass-to-light-ratio include (a) assuming the scatter between halo mass and UV magnitude increases at high redshift, possibly due to large fluctuations in the star formation rate (e.g., Ren, Trenti & Mason 2019; Mason, Trenti & Treu 2023; Shen et al. 2023; Sun et al. 2023; Kravtsov & Belokurov 2024), (b) a decrease in the dust attenuation of high-redshift massive galaxies as a result of strong radiation pressure (Ferrara, Pallottini & Dayal 2023), (c) modifying the stellar initial mass function by, for example, making it more top-heavy (e.g. Yung et al. 2024, although cf. Cueto et al. 2024), and (d) an increased role of nebular continuum emission due to, for example, intense star formation events and/or hotter or more massive stars (Katz et al. 2024). Alternatively, some simulations and models demonstrate that the star formation efficiency may be higher in the early Universe due to weaker feedback and strong gas inflows (e.g., McCaffrey et al. 2023; Dekel et al. 2023).

The variety of proposed solutions are not mutually exclusive — the underlying physical origin of both the excess UV luminosity density and number density of high-redshift bright galaxies is likely a combination of multiple factors. However, theoretical predictions for UV luminosities inevitably rely on stellar population synthesis (SPS) models such as STARBURST99 (Leitherer et al. 1999), BPASS (Stanway & Eldridge 2018), or BC03 (Bruzual & Charlot 2003). The predicted luminosities of the SPS models are subject to certain underlying assumptions, for example, chemical abundance ratios. It is typically assumed that metal abundance ratios are independent of metallicity and that the helium abundance is close to the value of $Y = 0.241$ as measured from the CMB (Planck Collaboration et al. 2020) with perhaps a slight excess that increases with metallicity.

However, spectroscopic observations from JWST have revealed that the chemical abundance patterns in numerous high-redshift galaxies are distinctly non-solar. Most-notably, a class of galaxies has been identified that exhibit strong rest-frame UV nitrogen emission lines (e.g., Cameron et al. 2023; Bunker et al. 2023; Isobe et al. 2023; Senchyna et al. 2024; Castellano et al. 2024; Topping et al. 2024b,a; Schaerer et al. 2024). Interestingly, three of these galaxies are at $z > 9$, with GNz11 and GHZ2 being two of the brightest spectroscopically confirmed objects in the sky at these redshifts. Numerous studies have highlighted the similarity between the gas-phase nitrogen abundances in these high-redshift nitrogen-emitters and stellar abundance patterns found in local globular clusters (e.g., Senchyna et al. 2024; Charbonnel et al. 2023; Marques-Chaves et al. 2024). Assuming this connection is causal and based on stars in the Milky Way, Belokurov & Kravtsov (2023) estimated that $50-70\%$ of star formation in our galaxy likely occurs in massive, bound clusters with properties similar to globular clusters, prior to disk formation.

One of the unique signatures of globular clusters is

their peculiar chemical abundance patterns (e.g., Bastian & Lardo 2018). The fraction of nitrogen-enriched stars scales with the cluster initial mass (Milone et al. 2017; Gratton et al. 2019; Belokurov & Kravtsov 2023; Usman et al. 2024) as does the enhancement in helium above the value expected from Big Bang nucleosynthesis (Milone et al. 2018; Gratton et al. 2019). For certain Milky Way globular clusters (e.g., Omega Centauri, NGC 2808) the helium mass fraction can reach as high as $Y \sim 0.4$ (Norris 2004; Piotto et al. 2005; Dupree & Avrett 2013; Joo & Lee 2013; Pasquini et al. 2011). Other Milky Way globular clusters also show helium enhancements (e.g. Caloi & D'Antona 2007; Busso et al. 2007; Dalessandro et al. 2013), albeit less extreme than Omega Centauri and NGC 2808. Similar helium enhancements have also been observed in the Galactic bulge (Renzini 1994; Nataf et al. 2011). Such helium enhancements up to $Y \sim 0.4$ have now been observed at high redshift ($z \sim 6$) in the gas phase alongside the aforementioned nitrogen enhancements (Yanagisawa et al. 2024), further tightening the link between these high-redshift nitrogen emitters and local globular clusters.

In this Letter, we simply highlight the fact that an increased helium mass fraction naturally increases both the luminosity and temperature of stars. If a large fraction of high-redshift star formation occurs in dense, bound clusters as suggested by both Milky Way data (Belokurov & Kravtsov 2023) and high-redshift gravitationally lensed objects (e.g., Vanzella et al. 2022; Adamo et al. 2024; Fujimoto et al. 2024; Mowla et al. 2024), then significant helium enrichment and consequent luminosity enhancement may be a natural byproduct. Here, we quantify the excess luminosity one may expect for a helium-enriched population of stars and discuss how this may help relieve some of the tension regarding the excess UV luminosity at high redshift.

2. THE IMPACT OF HELIUM ENHANCEMENTS ON 1500 Å UV LUMINOSITIES

It is well established that both the total bolometric luminosity of a star and its effective temperature are sensitive to both mean molecular weight (μ) and opacity (κ). For a star in radiative equilibrium with an ideal gas equation of state, the bolometric luminosity (L) scales as (see, e.g., Lamers & Levesque 2017):

$$L \propto \frac{\mu^4 M^3}{\kappa}. \qquad (1)$$

For stars with $M > 2\ \mathrm{M_\odot}$ where electron scattering represents the dominant opacity, $\kappa \propto 1 + X$, where X is the mass fraction of hydrogen. Ignoring metals and assuming a fully ionized medium, $\kappa \to 2 - Y$ and $\mu \to (2 - \frac{5}{4}Y)^{-1}$ such that at constant mass,

$$L \propto \frac{1}{(2 - \frac{5}{4}Y)^4(2 - Y)}. \qquad (2)$$

In Figure 1 (green line) we show the bolometric luminosity of a fixed-mass star, subject to the above-listed assumptions, scaled to the luminosity assuming Big Bang Nucleosynthesis (BBN) abundances ($Y = 0.24$, Planck Collaboration et al. 2020). For the maximum helium abundance seen in Omega Centauri (Dupree & Avrett 2013) and observed in the $z \sim 6$ galaxy RXCJ2248-ID
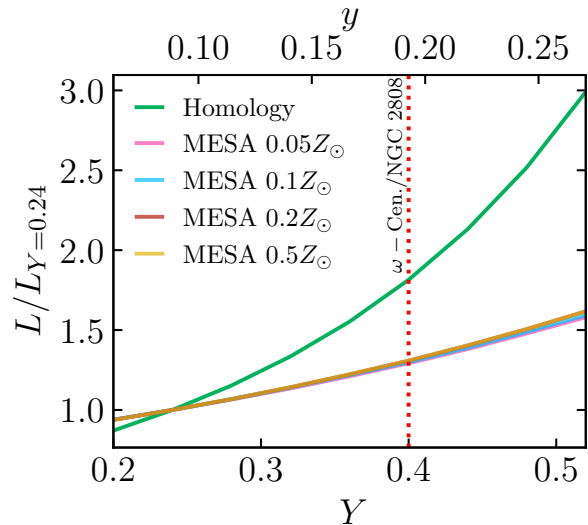

FIG. 1.— (Green) Bolometric luminosity of a fixed-mass star as a function of helium mass fraction (Y), scaled to the value assuming a BBN helium abundance ($Y = 0.24$). This model assumes that the star is in radiative equilibrium, that the gas is fully-ionized and metal free, and that the opacity is dominated by electron scattering. (Pink, Blue, Brown, Yellow) 1500 Å luminosity integrated over a Salpeter IMF as computed with MESA at $Z = 0.05Z_\odot$, $0.1Z_\odot$, $0.2Z_\odot$, and $0.5Z_\odot$, respectively, scaled to the value assuming a BBN helium abundance. In both cases, the luminosity is strongly sensitive to Y. For reference, the dotted red line indicates $Y = 0.4$, which represents the maximum helium abundances seen in Milky Way globular clusters Omega Centauri and NGC 2808.

(Topping et al. 2024b; Yanagisawa et al. 2024), the bolometric luminosity increases by a factor of $\sim 80\%$.

Stars are of course more complex than this simple model based on homology encapsulates. To gain a more accurate estimate for the luminosity increase specifically at 1500 Å, we have run a series of MESA models (Paxton et al. 2011, 2013, 2015, 2018, 2019, Version r15140) to obtain the effective temperature and bolometric luminosity of the zero-age main-sequence (ZAMS) for different initial metallicities and values of Y. Our models supplement those in the literature (e.g. Karakas, Marino & Nataf 2014; Karakas 2014; Chantereau, Charbonnel & Decressin 2015; Chantereau, Charbonnel & Meynet 2016) that are typically run at a specific metallicity to focus on an individual globular cluster or environment. Models from $1 - 100\ M_\odot$ were run using the pp_and_cno_extras network and stopped when the hydrogen burning luminosity was within 0.1% of the total luminosity. Assuming the spectrum of each star follows a blackbody with $T = T_{\mathrm{eff}}$, we integrate the total luminosity at 1500 Å over a Salpeter (1955) IMF with a maximum mass of 100 $M_\odot$. The pink, blue, and brown, and yellow lines in Figure 1 shows the 1500 Å luminosity as a function of Y, normalized by the luminosity at $Y = 0.24$ for four different metallicities. Indeed the UV luminosity also increases with Y, although less steeply than our simple assumptions predict. Nevertheless, at $Y = 0.4$, the UV luminosity is still boosted by 30%. The relation between helium mass fraction, Y, and the luminosity excess at the ZAMS for our assumptions of IMF and $0.1Z_\odot$ is well fit by the relation:
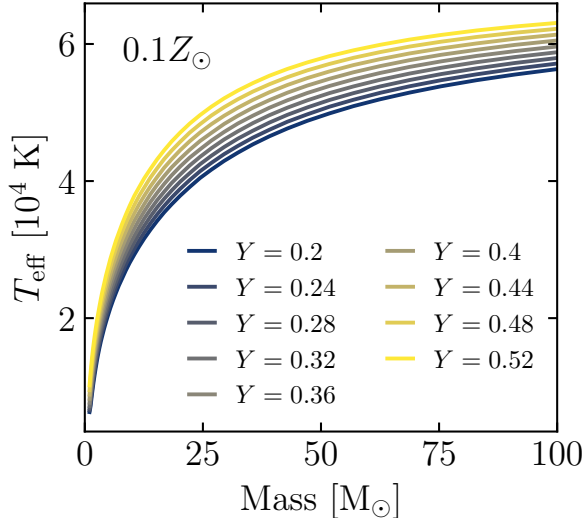
$$L/L_{Y=0.24} = 1.94Y^2 + 0.63Y + 0.74. \qquad (3)$$

FIG. 2.— Effective temperature as a function of zero-age main-sequence stellar mass for various helium mass fractions at a metallicity of $0.1Z_\odot$. Higher values of Y lead to hotter stars. This behavior is consistent across all metallicities in our grid.

FIG. 3.— Bolometric luminosity of individual stars at the ZAMS as a function of mass for different values of Y, normalized to the values at the same mass for $Y = 0.24$. Lower-mass stars are more affected by higher values of Y. We show results for a metallicity of $0.1Z_\odot$; however, other metallicities exhibit similar behavior. Note that the wiggles in the plot are likely numerical due to the finely sampled mass grid.

Unfortunately, helium abundance measurements are not possible for the highest-redshift nitrogen emitters due to the He^+ recombination lines (particularly $He\,I\,\lambda7065$) dropping out of the JWST NIRSpec prism at $z \gtrsim 6.5$. To estimate Y for GNz11 (Bunker et al. 2023), GHZ2 (Castellano et al. 2024), and GN-z9p4 (Schaerer et al. 2024), we fit an empirical relation between $\log(N/O)$ and $y = He/H$ to the data presented in Yanagisawa et al. (2024) (their Figure 5) such that $y = 0.085e^{(\log(N/O)+1.6)^{2.7}/2.5}$. This gives $y > 0.21$ ($Y > 0.47$) for GNz11 using the fiducial value of N/O from Cameron et al. (2023), $0.19 < y < 0.23$ ($0.43 < Y < 0.48$) for GHZ2 using the various N/O estimated from Castellano et al. (2024), and $y = 0.13$ ($Y = 0.34$) for GN-z9p4 using the N/O measured from Schaerer et al. (2024). Assuming a Salpeter IMF and a metallicity of $0.1Z_\odot$, this would correspond to luminosity boosts of $> 43\%$, up to 48%, and 18%, for GNz11, GHZ2, GN-z9p4, respectively (following Equation 3).

Another consequence of an increased helium abundance is that the stellar effective temperature rises. Following from our previous assumptions, homology relations predict $T \propto \mu M/R$, where R is the radius of the star. The increase in temperature is indeed related to the increase in bolometric luminosity. Figure 2 highlights the impact of helium enhancement on the ZAMS $T_{\rm eff}$ in the same set of MESA models, which approach $\Delta T_{\rm eff}$ of 10 kK for $\gtrsim 25$ $M_\odot$ stars for the highest enhancements considered. To first order, hotter, more luminous stars have increased production of ionizing photons and their spectra are harder. It is important to consider that for real stars the exact details of this behavior depend on complex stellar atmosphere physics, which is beyond the scope of this letter. However, a higher ionizing photon production efficiency would lead, in an ionization-bounded nebula, to more nebular continuum emission, which also boosts UV luminosity (e.g., Raiter, Schaerer & Fosbury 2010; Katz et al. 2024). Moreover, harder photons may help power the observed C IV and N IV] emission lines, which are not
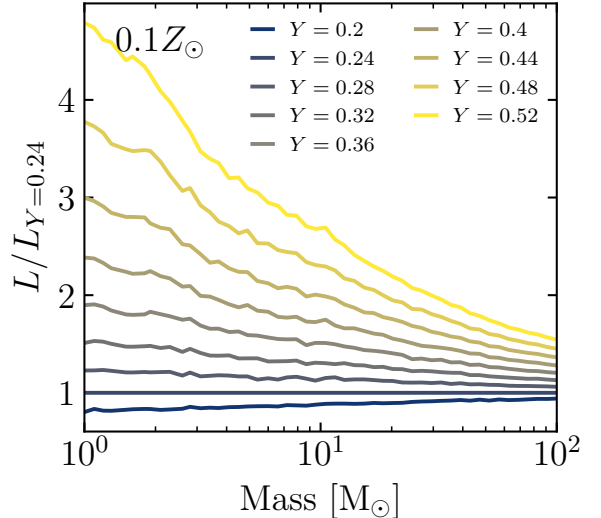
typically seen at such strengths in star-forming galaxies at lower redshifts even at similar metallicities (e.g., Senchyna et al. 2019; Berg et al. 2019; Izotov et al. 2024).

Finally, it is important to highlight that the impact on the total bolometric luminosity is not constant with mass. This is demonstrated in Figure 3, where we show the bolometric luminosity of individual stars at the ZAMS as a function of mass for different values of Y, normalized to the values at the same mass for $Y = 0.24$, assuming a metallicity of $0.1Z_\odot$. We observe that lower-mass stars exhibit larger increases in bolometric luminosity for all values of Y compared to higher-mass stars. This effect can be understood from homology relations. The highest mass stars have non-negligible contributions from radiation pressure to their equation of state. For a star entirely dominated by radiation pressure, at fixed mass, $L \propto (2 - Y)^{-1}$. At masses $\lesssim 2$ $M_\odot$, free-free and bound-free absorption contribute to the opacity where it can be shown that $L \propto \mu^{7.5}$. Because the impact of helium enhancements is mass-dependent, the evolution of properties such as mass-to-light ratio and when spectral features such as the Balmer break appear as a function of time may change and complicate estimates of stellar mass or star formation histories. These again depend on detailed calculations of stellar atmospheres and main-sequence lifetimes, but the effects may be relevant for interpreting the light from early galaxies impacted by globular cluster populations and other densely clustered star formation at a broad range of ages, in addition to the very young UV N-emitters that we have focused on in this work.

3. DISCUSSION & CONCLUSIONS

Here we have highlighted the fact that helium enhancements, which empirically scale strongly with N/O (Yanagisawa et al. 2024), lead to a boost in UV luminosity of individual stars due to the strong scaling of luminosity with mean molecular weight. For the nitro-

gen emitters observed at $z > 10$, detailed stellar evolution models predict that the 1500 Å UV luminosity can increase as much as $\sim 50\%$. This effect is likely to take place only in compact star-forming regions undergoing extreme bursts that exhibit similar conditions to what is expected for globular cluster 'second population' formation. Such galaxies represent $\sim 50\%$ of the very UV-bright population at high redshift, while the others are potentially mergers (e.g., Harikane et al. 2024). Thus the combination of an intense burst of star formation along with the luminosity increase from an enhanced helium abundance and strong nebular continuum could help explain why there exists a population of compact, very UV-bright galaxies at high redshift. Moreover, if a significant fraction of high-redshift star formation occurs in massive star clusters as predicted from Milky Way data (Belokurov & Kravtsov 2023), helium enhancements may be more common at high-redshift than in the local Universe; and could contribute to the general excess UV luminosity density as well as impact retrieval of stellar masses and ages for affected systems.

REFERENCES

Adamo A. et al., 2024, Nature, 632, 513
Bastian N., Lardo C., 2018, ARA&A, 56, 83
Belokurov V., Kravtsov A., 2023, MNRAS, 525, 4456
Berg D. A., Chisholm J., Erb D. K., Pogge R., Henry A., Olivier G. M., 2019, The Astrophysical Journal, 878, L3
Bruzual G., Charlot S., 2003, MNRAS, 344, 1000
Bunker A. J. et al., 2023, A&A, 677, A88
Busso G. et al., 2007, A&A, 474, 105
Caloi V., D'Antona F., 2007, A&A, 463, 949
Cameron A. J., Katz H., Rey M. P., Saxena A., 2023, MNRAS, 523, 3516
Castellano M. et al., 2024, arXiv e-prints, arXiv:2403.10238
Chantereau W., Charbonnel C., Decressin T., 2015, A&A, 578, A117
Chantereau W., Charbonnel C., Meynet G., 2016, A&A, 592, A111
Charbonnel C., Schaerer D., Prantzos N., Ramírez-Galeano L., Fragos T., Kuruvanthodi A., Marques-Chaves R., Gieles M., 2023, A&A, 673, L7
Chemerynska I. et al., 2023, arXiv e-prints, arXiv:2312.05030
Cueto E. R., Hutter A., Dayal P., Gottlöber S., Heintz K. E., Mason C., Trebitsch M., Yepes G., 2024, A&A, 686, A138
Dalessandro E., Salaris M., Ferraro F. R., Mucciarelli A., Cassisi S., 2013, MNRAS, 430, 459
Dekel A., Sarkar K. C., Birnboim Y., Mandelker N., Li Z., 2023, MNRAS, 523, 3201
Dupree A. K., Avrett E. H., 2013, ApJ, 773, L28
Ferrara A., Pallottini A., Dayal P., 2023, MNRAS, 522, 3986
Finkelstein S. L. et al., 2023, arXiv e-prints, arXiv:2311.04279
Fujimoto S. et al., 2024, arXiv e-prints, arXiv:2402.18543
Gardner J. P. et al., 2006, Space Sci. Rev., 123, 485
Gratton R., Bragaglia A., Carretta E., D'Orazi V., Lucatello S., Sollima A., 2019, A&A Rev., 27, 8
Harikane Y., Nakajima K., Ouchi M., Umeda H., Isobe Y., Ono Y., Xu Y., Zhang Y., 2024, ApJ, 960, 56
Isobe Y. et al., 2023, ApJ, 959, 100
Izotov Y. I., Schaerer D., Guseva N. G., Thuan T. X., Worseck G., 2024, Monthly Notices of the Royal Astronomical Society, 528, L10
Joo S.-J., Lee Y.-W., 2013, ApJ, 762, 36
Karakas A. I., 2014, MNRAS, 445, 347
Karakas A. I., Marino A. F., Nataf D. M., 2014, ApJ, 784, 32
Katz H. et al., 2024, arXiv e-prints, arXiv:2408.03189
Kravtsov A., Belokurov V., 2024, arXiv e-prints, arXiv:2405.04578

Lamers H. J. G. L. M., Levesque E. M., 2017, Understanding Stellar Evolution
Leitherer C. et al., 1999, ApJS, 123, 3
Leung G. C. K. et al., 2023, ApJ, 954, L46
Marques-Chaves R. et al., 2024, A&A, 681, A30
Mason C. A., Trenti M., Treu T., 2023, MNRAS, 521, 497
McCaffrey J., Hardin S., Wise J. H., Regan J. A., 2023, The Open Journal of Astrophysics, 6, 47
Milone A. P. et al., 2018, MNRAS, 481, 5098
Milone A. P. et al., 2017, MNRAS, 464, 3636
Mowla L. et al., 2024, arXiv e-prints, arXiv:2402.08696
Nataf D. M., Udalski A., Gould A., Pinsonneault M. H., 2011, ApJ, 730, 118
Norris J. E., 2004, ApJ, 612, L25
Pasquini L., Mauas P., Käufl H. U., Cacciari C., 2011, A&A, 531, A35
Paxton B., Bildsten L., Dotter A., Herwig F., Lesaffre P., Timmes F., 2011, ApJS, 192, 3
Paxton B. et al., 2013, ApJS, 208, 4
Paxton B. et al., 2015, ApJS, 220, 15
Paxton B. et al., 2018, ApJS, 234, 34
Paxton B. et al., 2019, ApJS, 243, 10
Piotto G. et al., 2005, ApJ, 621, 777
Planck Collaboration et al., 2020, A&A, 641, A6
Raiter A., Schaerer D., Fosbury R. A. E., 2010, A&A, 523, A64
Ren K., Trenti M., Mason C. A., 2019, ApJ, 878, 114
Renzini A., 1994, A&A, 285, L5
Salpeter E. E., 1955, ApJ, 121, 161
Schaerer D., Marques-Chaves R., Xiao M., Korber D., 2024, A&A, 687, L11
Senchyna P., Plat A., Stark D. P., Rudie G. C., Berg D., Charlot S., James B. L., Mingozzi M., 2024, ApJ, 966, 92
Senchyna P., Stark D. P., Chevallard J., Charlot S., Jones T., Vidal-García A., 2019, Monthly Notices of the Royal Astronomical Society, 488, 3492
Shen X., Vogelsberger M., Boylan-Kolchin M., Tacchella S., Kannan R., 2023, MNRAS, 525, 3254
Stanway E. R., Eldridge J. J., 2018, MNRAS, 479, 75
Sun G., Faucher-Giguère C.-A., Hayward C. C., Shen X., Wetzel A., Cochrane R. K., 2023, ApJ, 955, L35
Topping M. W. et al., 2024a, arXiv e-prints, arXiv:2407.19009
Topping M. W. et al., 2024b, MNRAS, 529, 3301
Usman S. A. et al., 2024, MNRAS, 529, 2413
Vanzella E. et al., 2022, ApJ, 940, L53
Willott C. J. et al., 2023, arXiv e-prints, arXiv:2311.12234

Yanagisawa H. et al., 2024, arXiv e-prints, arXiv:2405.01823

Yung L. Y. A., Somerville R. S., Finkelstein S. L., Wilkins S. M., Gardner J. P., 2024, MNRAS, 527, 5929

This paper was built using the Open Journal of Astrophysics LaTeX template. The OJA is a journal which provides fast and easy peer review for new papers in the `astro-ph` section of the arXiv, making the reviewing process simpler for authors and referees alike. Learn more at http://astro.theoj.org.